Originally published (in Russian):
Kutakov M.N., Degtiarev S.A., Leontiev M.K. Mathematical models of squeeze film dampers in rotor dynamics of gas turbine engines. Vestnik of Samara University. Aerospace and Mechanical Engineering. 2017. V. 16, no. 1. P. 115-128. DOI: 10.18287/2541-7533-2017-16-1-115-128

MATHEMATICAL MODELS OF SQUEEZE FILM DAMPER IN GAS TURBINE ENGINE ROTOR SUPPORT.

Kutakov M.N.[1], Degtiarev S.A.[1], Leontiev M.K.[2]
[1]Engineering & consulting centre for dynamic problems in rotating machinery Alfa-Tranzit., Co. Ltd., Khimky, Russia
[2]Moscow aviation institute (national research university), Moscow, Russia

Abstract
The papers focuses the choice of mathematical models of squeeze film dampers and methods their numerical implementations for gas turbine engines rotor dynamics problems. The present contribution is aimed to establish criteria when or another squeeze film damper formulation should be used, depending on the damper characteristics and operating conditions. The models are grouped by the dimension of the considered physical space, i.e. three-dimensional, two-dimensional and one-dimensional modelling patterns. The work presents the boundary conditions for mechanical seals to be adequately simulated. The numerical estimates for necessity of taking into account such physical phenomena as turbulence, fluid inertia, and cavitation are disclosed. The presented mathematical models are primarily developed for the computation of the integral characteristics of squeeze film dampers, such as reaction forces and dynamic stiffness and damping coefficients, required for solving rotor dynamics problems.
Key words: *tribology, hydrodynamics, mathematical model, squeeze film damper*

Introduction

The Squeeze Film Dampers (SFD) are widely used in aero Gas Turbine Engines (GTE) rotor supports. SFD application reduces GTE vibration levels, bearing support loads, stress in GTE parts and assemblies. Numerous papers are concerned with analysis and experimental investigation of the SFD fluid flow and SFD design in rotor systems. SFD simulation and design topics may be found in papers [1 – 4].

Nevertheless, the SFD design, simulation and work analysis are still considered as complicated rotor system elements. In authors understanding introduction SFD into a GTE rotor computer model still the most complicated task. Now all advanced rotordynamics analysis software sets include simulation of rotors with SFD supports, more or less reflecting the actual object. Correct application of these tools is the user's problem.

The SFD model for a rotordynamics system is based on simulation of fluid flow in the damper clearance. The model must conform to the object together with minimal calculation amount needed for computation of forced performance parameters, which are required for the rotor system dynamics numerical modeling.

Squeeze film damper model

A principal hydrodynamic damper (fig. 1) is formed by cylindrical surfaces of a quill, or exciter, and the damper housing. The quill is fixed on the bearing outer ring or housing. The exciter does not rotate but travels together with the shaft in the whirling motion.

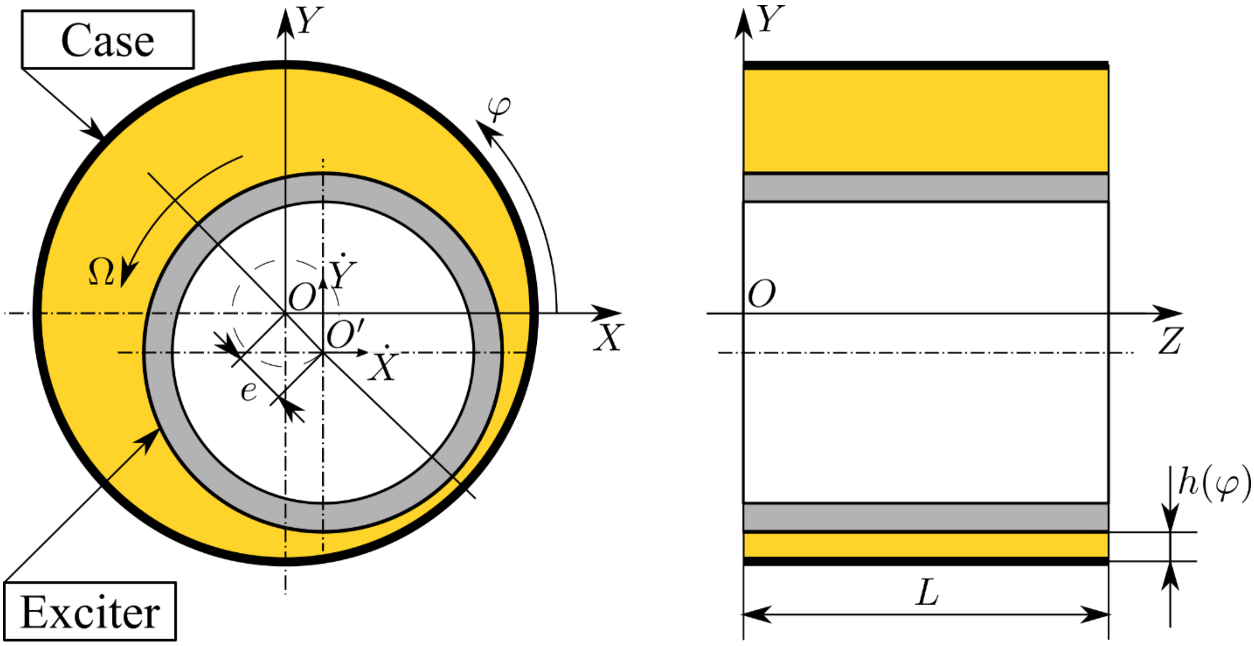

Fig. 1. Squeeze film damper principal scheme.

In general, for an incompressible, isoviscous Newtonian fluid, laminar flow may be described by Navier-Stoks and continuity, or mass conservation, equations that may be presented in the vector form [5]:

$$\begin{cases} \mathrm{div}(\bar{v}) = 0; \\ \rho \dfrac{\mathrm{d}\,\bar{v}}{\mathrm{d}\,t} = -\mathrm{grad}(p) + \mathrm{div}(2\mu D) + \rho \bar{f}, \end{cases} \tag{1}$$

here $\bar{v}$ – velocity vector, ρ - specific mass, p – static pressure, $\bar{f}$ – body force vector, D – stretching tensor.

System (1) involves partial differential equations, which may be numerically solved including boundary and initial conditions with special tools, finite element, or finite volume methods, etc. [6]. Many code sets are concerned to hydrodynamics problems, both commercial, like ANSYS CFX, Fluent, or open source, OpenFOAM, CodeSaturn, etc. that may be used for this problem. For example, paper [7] describes SFD simulation with the CFD code of ANSYS CFX. The acceptable simulation accuracy could be reached at about 10^6 degrees of freedom, which is not crucial by itself but requires a remarkable calculation time. The result is a 3D flow pattern in the damper clearance. Available CFD tools allow description of the most specific features, turbulence, cavitation, temperature distortions, heat exchange with walls, at minimal set of assumptions. CFD is the full and potentially accurate practical simulation tool but its calculation amount is very large.

The fundamental dimensional feature of the dampers may simplify the problem, the damper clearance is much smaller than all other damper dimensions, exciter circle length and width.

$$\varepsilon = \frac{c}{R} = \boldsymbol{O}\,(10^{-3}), \tag{2}$$

here c – nominal damper clearance, R – exciter radius. In 1866 under the assumption (2) Reynolds [8] obtained an equation that describes also sleeve bearings. A few assumptions are also involved here:

a. The fluid is incompressible,
b. The liquid viscosity is constant throughout the volume,
c. The fluid inertia is negligible,

d. Turbulence effects are not considered.

In the polar coordinates, this equation may describe the fluid film flow.

$$\frac{\partial}{R^2\partial\varphi}\left(\frac{h^3}{12\mu}\frac{\partial p}{\partial\varphi}\right)+\frac{\partial}{\partial z}\left(\frac{h^3}{12\mu}\frac{\partial p}{\partial z}\right)=\frac{\partial h}{\partial t}+\frac{1}{2}\omega\frac{\partial h}{\partial\varphi}, \quad (3)$$

here R – shaft neck radius, μ – dynamic viscosity, h - radial clearance between the shaft neck and the housing, ω – shaft neck rotation speed, φ, z – angular and axial coordinates, p – pressure. Derivation of Reynolds equation from (1) is completely described, for example in [5].

On the contrary to sleeve bearings in dampers the shaft neck rotation is blocked, or its angular speed is 0, then:

$$\frac{\partial}{R^2\partial\varphi}\left(\frac{h^3}{12\mu}\frac{\partial p}{\partial\varphi}\right)+\frac{\partial}{\partial z}\left(\frac{h^3}{12\mu}\frac{\partial p}{\partial z}\right)=\frac{\partial h}{\partial t}. \quad (4)$$

The exciter and the housing are two parallel cylinders, their axes misalignment is not considered. Then the circular clearance distribution is the following:

$$h(\varphi)=c-X\cos(\varphi)-Y\sin(\varphi), \quad (5)$$

$$\frac{\partial h}{\partial t}=-\dot{X}\cos(\varphi)-\dot{Y}\sin(\varphi), \quad (6)$$

here X, Y – exciter center coordinates, $\dot{X}, \dot{Y}$ – exciter center velocity. Equation (4) looks as

$$\frac{\partial}{R^2\partial\varphi}\left(\frac{h^3}{12\mu}\frac{\partial p}{\partial\varphi}\right)+\frac{\partial}{\partial z}\left(\frac{h^3}{12\mu}\frac{\partial p}{\partial z}\right)=-\dot{X}\cos(\varphi)-\dot{Y}\sin(\varphi). \quad (7)$$

The partial differential equation (7) is elliptic in relation to p. Its solution requires boundary conditions that may be obtained from the object physical nature. A simple cylindrical damper evolvent (fig. 2) may be presented as the rectangular computational domain Ω.

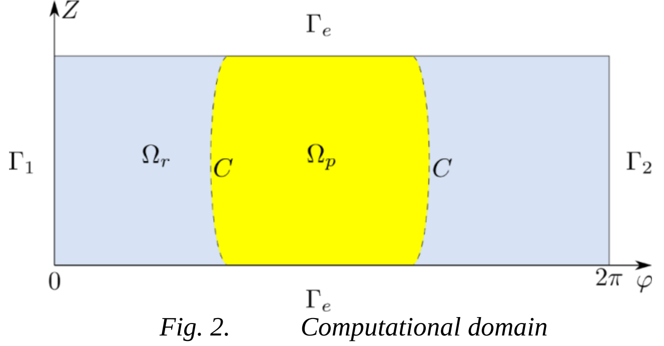

Fig. 2. Computational domain

The computational domain closed, so the boundary conditions for borders Γ_1, Γ_2 must be periodic:

$$\begin{cases} \left.\frac{\partial p}{\partial \bar{n}}\right|_{\Gamma_1}+\left.\frac{\partial p}{\partial \bar{n}}\right|_{\Gamma_2}=0; \\ p_{\Gamma_1}=p_{\Gamma_2}, \end{cases} \quad (8)$$

here $\bar{n}$ is normal to the border. The end seals type determines boundary conditions on edges Γ_e. Versions of end seals are shown in fig. 3.

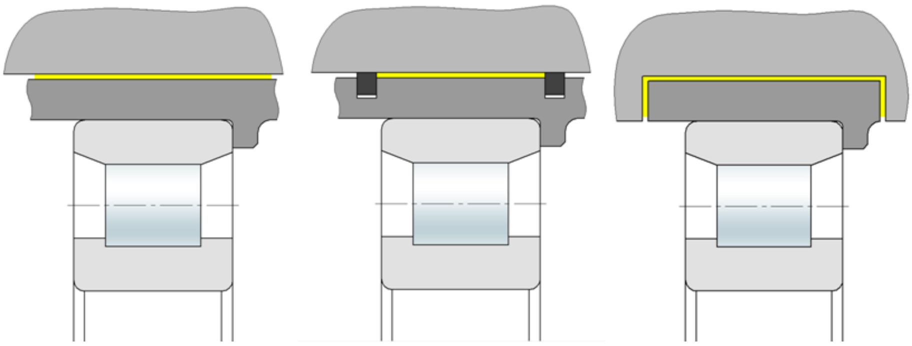

Fig. 3. Types of damper end seals: a) open ends, b) piston rings, c) clearance gap seals.

In the open ends damper (fig. 3 a) the boundary condition is the ambient pressure, usually the normal atmospheric, or zero excessive. Then the boundary condition is:

$$p(\varphi)\big|_{\Gamma_e} = p_a = 0, \tag{9}$$

here p_a is the ambient pressure. In the sealed damper (fig. 3 b) the perfect case is no leakage through the end seals, and this boundary condition is:

$$\left.\frac{\partial p}{\partial \bar{n}}\right|_{\Gamma e} = 0. \tag{10}$$

In the clearance gap sealed damper the boundary condition is:

$$\left.\frac{h^3}{12\mu}\frac{\partial p}{\partial \bar{n}}\right|_{\Gamma e} = q, \tag{11}$$

here $q = f(p)$ - volumetric oil flow through the seal determined by the pressure drop and the seal hydraulic resistance. The end leakage in fig. 3 b) type damper the boundary condition (11) may be applied. The conditions (8) to (11) are sufficient for the equation (7).

In realistic conditions dampers may meet effects of gas or vapor cavitation. Experimental investigation of the cavitation effect described in paper [9]. Gas cavitation effect is separation from the fluid of the gas dissolved in this fluid at pressures below the gas equilibrium. Steam cavitation effect is the fluid boiling at pressures below the saturation vapor pressure. In oil the saturation vapor pressure is usually lower than the dissolved gas equilibrium, so the gas cavitation is more usual. Besides this when the oil film pressure is below the ambient pressure the surrounding gas may penetrate into the low pressure zone. As to consider the cavitation effect the cavitation conditions C must be added to the boundary conditions.

$$\begin{aligned} &C = \partial\Omega_r \cap \partial\Omega_p; \\ &\Omega_r \overset{\Delta}{=} \{x \in \Omega \mid p(x) = 0\}; \\ &\Omega_p \overset{\Delta}{=} \{x \in \Omega \mid p(x) > 0\}. \end{aligned} \tag{12}$$

Approaches to cavitation zone simulation may be found in papers [10,11]. The simplest application is Gumbel boundary condition that assumes the oil film rupture at a negative pressure. Equation (7) is solved in the computational domain Ω and the negative pressure is assumed equal to zero:

$$p(x) < 0 \rightarrow p(x) = 0. \tag{13}$$

The Gumbel boundary conditions don't provide volumetric flow conservation. The Swift – Stieber boundary conditions (sometimes referred as Reynolds boundary conditions) provide volumetric flow conservation at the cavitation zone border:

$$\left.\frac{\partial p}{\partial \bar{n}}\right|_C = 0, \quad p(x)\,|_C = 0. \tag{14}$$

The Swift – Stieber conditions do not provide mass flow conservation and determine the cavitation zone only approximately. The mass flow is kept in other models, for example Jakobsson-Floberg-Olsson, Elrod cavitation models. Nevertheless, the boundary conditions (14) are widely used in practical analysis.

Equation (7) with boundary conditions (8) – (11) or (14) may be solved with numerical methods, for example in finite differences, or finite elements, or finite volume. The problem solution dimension will be from a few hundred to a few thousand degrees of freedom, which is remarkably smaller than the CFD simulation. The Reynolds equation may be applied only to thin films which is sufficient for most of the damper calculations. Specific elements like the oil distribution groove that is much deeper than the damper clearance need a special consideration. Besides this a special attention must be paid to limits the base assumptions application.

A flow in the fluid film may be of two types, laminar or turbulent. In the laminar flow the viscous forces prevail and mitigate all random flow fluctuations. When inertia effects overcome viscous ones and the flow amplifies random fluctuations the flow mode is turbulent. The flow mode may be determined by the Reynolds criteria that specifies the ratio of inertia and viscous forces. In dampers the circular flow velocity is determined by the shear flow caused by the exciter motion. Usually the shear flow velocity in circular direction is larger than the pressure flow velocity to the film ends direction. Then the turbulence occurrence may be specified with the shear flow Reynolds number [3, p. 282]:

$$Re = \frac{\rho R \Omega e}{\mu}, \tag{15}$$

where Ω - exciter oscillation frequency, e - exciter eccentricity. It is possible to assume that a flow is laminar if the Reynolds number is below its critical value. Experiments have estimated the critical value of damper Reynolds number as $Re_k \approx 1200$ [3, 12]. The turbulence occurrence may remarkably influence the flow and must be taken into account.

The turbulence may be considered by the modified Reynolds equation with turbulence correction coefficients k_x, k_z.

$$\frac{\partial}{R^2 \partial \varphi}\left(\frac{h^3}{k_x \mu}\frac{\partial p}{\partial \varphi}\right) + \frac{\partial}{\partial z}\left(\frac{h^3}{k_z \mu}\frac{\partial p}{\partial z}\right) = -\dot{X}\cos(\varphi) - \dot{Y}\sin(\varphi). \tag{16}$$

The correction coefficients k_x, k_z are calculated with the following thin film turbulence models:

- Constantinescu's turbulence model for thin film flows is based on the Prandtl mixing length hypothesis,
- Ng-Pan-Elrod model based on the Reichardt - Clauser equations,
- Ho-Vohr model based on the turbulence k-model,
- Launder-Leschziner k – ε model for sleeve bearings,
- Hirs, Black and Walton empirical drag laws.

The fluid inertia force placed in the left part of Navier-Stocks equation (1).

$$\rho\frac{\mathrm{d}\,\bar{v}}{\mathrm{d}\,t}=\rho\left(\frac{\partial\bar{v}}{\partial t}+\bar{v}\cdot\nabla\bar{v}\right)=-\mathrm{grad}(\,p)+\mathrm{div}(2\mu D)+\rho\bar{f}\,. \tag{17}$$

The components in brackets are called inertia components, temporal $\rho\frac{\partial\bar{v}}{\partial t}$ and convective $\rho\bar{v}\cdot\nabla\bar{v}$. The temporal inertia forces are caused by the fluid in clearance acceleration and may be remarkable at accelerated exciter motion. Thus these temporal inertia components are taken into account in unsteady problems. The convective components reflect local fluid accelerations and have smaller influence upon the damper performance [3]. They must be considered in steady state problems at small temporal inertia forces are combined with high rotation speeds and for low viscosity fluids [1].

In sleeve bearings two parameters may determine the inertia influences upon the final result [5], reduced frequency Ω_* and reduced Reynolds number R_ε:

$$R_\varepsilon=\left(\frac{c}{R}\right)Re, \tag{18}$$

$$\Omega_*=\frac{c^2\Omega\rho}{\mu}. \tag{19}$$

The inertia components in equation (1) in thin films influence the final results at $\Omega_*>1$ and $R_\varepsilon>1$. Here the three cases to be considered are the following:

1. $R_\varepsilon/\Omega_*\to 0$, $\Omega_*>1$– only the temporal inertia component to be considered,
2. $\Omega_*/R_\varepsilon\to 0$, $R_\varepsilon>1$ - only the convective inertia component
3. $\Omega_*/R_\varepsilon\to \boldsymbol{O}(1)$, $R_\varepsilon>1$ - the both components to be considered,

In dampers the shaft does not rotate, so R_ε and Ω_* are generally the same numbers. In other works [1] this parameter is called inertia parameter, or squeeze film Reynolds number [13].

The system (1) solution automatically includes the inertia forces. It is complicated to reduce system (1) to a type (4) equation with the convective inertia component. Are known different methods for the inertia forces involvement, for example the velocity averaging through the layer thickness [5, p. 213], but these methods are not considered here. The temporal inertia component may be included into the Reynolds equation right part [13]:

$$\frac{\partial}{R^2\partial\varphi}\left(\frac{h^3}{12\mu}\frac{\partial p}{\partial\varphi}\right)+\frac{\partial}{\partial z}\left(\frac{h^3}{12\mu}\frac{\partial p}{\partial z}\right)=\frac{\partial h}{\partial t}+\left(\frac{\rho h^2}{12\mu}\right)\frac{\partial^2 h}{\partial t^2}, \tag{20}$$

Based on experimental data [1] the authors assume that the convective inertia components must be taken into account at $\Omega_*>10$.

In dampers the oil film temperature non-uniformity mostly depends upon the following factors: heat release caused by the mechanical energy dissipation, oil flow through the damper and the housing temperature non-uniformity caused by its external heating. In open ends and clearance gap seal dampers a remarkable part of the produced heat is evacuated by the damper oil flow. In closed ends dampers the oil flow is small and the oil film temperature non-uniformity may occur. Analysis of this temperature non-uniformity requires additional solution of the energy conservation equation which remarkably complicates the problem. According to the assessment [1] absence of the temperature non-uniformity analysis may cause about 5% error, in sealed dampers the error may grow up to 60% at large eccentricity. The housing and exciter temperature non-uniformity may be taken from their heat analysis and also may influence the clearance oil flow. In this case it is necessary to consider the balance between the heat transfer between housing and oil flow and the amount of heat evacuated by the oil flow. Finally, in the open end dampers the temperature non-uniformity is negligible, the sealed clearance dampers need this analysis. In sealed dampers the error due to the absence of temperature non-uniformity analysis will be below 60% which is acceptable in many cases. In this paper we consider the average oil film temperature that gives correct values of the oil viscosity.

Equation (4) is not generally solved with the analytical approach but in some cases the calculation time is important. Two additional assumptions may provide analytical expressions for the fluid film pressure distribution that will be correct at definite conditions. First, we assume that the circular pressure gradient is much larger than the axial one. Then the $\partial p/\partial z$ component is negligible. This assumption is called “long damper” model, and it is correct at $L/D > 2$ [7]. For the “long” damper the Reynolds equation is:

$$\frac{\partial}{R^2\partial\varphi}\left(\frac{h^3}{12\mu}\frac{\partial p}{\partial\varphi}\right)=\frac{\partial h}{\partial t}+\left(\frac{\rho h^2}{12\mu}\right)\frac{\partial^2 h}{\partial t^2}, \tag{21}$$

The other assumption is the “short” damper model, i.e. the circular pressure gradient is smaller than the axial one. This assumption may be applied at $L/D < 0.5$ and eccentricity $\varepsilon \le 0.75$ [14]. For this case the Reynolds equation is:

$$\frac{\partial}{\partial z}\left(\frac{h^3}{12\mu}\frac{\partial p}{\partial z}\right)=\frac{\partial h}{\partial t}+\left(\frac{\rho h^2}{12\mu}\right)\frac{\partial^2 h}{\partial t^2}, \tag{22}$$

Equations (21) and (22) together with the boundary conditions (8) – (11) allow analytical solutions. It is important to note that above L/D range defined for open ends dampers (fig. 3 a) or equivalent ones (see details in reference [2]). In first assumption dampers with end seal can be considered like “long” without taking in to account L/D ratio, because in ideal case flow through seals consider equal to zero, therefore pressure gradient in z direction is also zero. Presence of circumferential feed grove leads to significant pressure gradient in axial direction and such damper could be considered like “short”. For a dampers with clearance gap seals (fig. 3 c) identification of applicability of analytical equations is difficult, because flow through seals and pressure gradient in axial direction strongly depends from end seal gap clearance and length. For these dampers two-dimensional Reynolds equation is preferred.

The “short” and “long” damper models are limited by the L/D ratio and are not used for the $0.5 < L/D < 2$ range. In this case is preferred the finite length damper model. For these dampers it is possible to solve the 2-D Reynolds equation that automatically takes into account both circular and axial flows, which gives potentially more accurate results than the 1-D models. Methods for analytical calculation of fluid inertia, cavitation and turbulence in “short” and “long” dampers discussed in reference [1].

The cavitation effect is an important aspect of the equations (21) and (22) analytical solutions. Application of the Swift-Stieber conditions is complicated, so in practice are usually applied so-called π - film, or Gumbel conditions that reflects the half covered exciter, or 2π - film, or Sommerfeld conditions that reflects the completely covered exciter without cavitation. The choice between the π - film and the 2π - film is up to the user who is to assume the cavitation zone presence. In closed dampers with high oil supply pressure the cavitation zone may occur at higher vibrator velocities and larger eccentricity than in open ends dampers with low oil supply pressure. The occurrence and size of cavitation region depends from oil supply pressure, presence of mechanical seals, speed and eccentricity of the exciter. Some parameters allow approximate assessment the cavitation occurrence. The book [1] summarizes numerical calculations of the cavitation parameters depending from eccentricity and oil supply parameters at the exciter circular whirling motion.

$$A_{\hat{E}} = 1 + (3.76(1-\varepsilon)^{1.51} \exp[2.89(1-\varepsilon)])\overline{P}_{\acute{E}} ,$$
$$B_{\hat{E}} = 1 - (10.2(1-\varepsilon)^{2.24} \exp[1.88(1-\varepsilon)])\overline{P}_{\acute{E}} , \qquad (23)$$

$$A'_{\hat{e}} = 1 + (1.1(1-\varepsilon)^{1.17} \exp[3.17(1-\varepsilon)])\overline{P}_{\acute{E}} ,$$
$$B'_{\hat{e}} = 1 - (5.84(1-\varepsilon)^{2.41} \exp[0.89(1-\varepsilon)])\overline{P}_{\acute{E}} , \qquad (24)$$

$$A_{\ddot{A}} = 1 + 4\times10^{-5}(1-\varepsilon)^{6.12} \exp[12.9(1-\varepsilon)]\overline{P}_N^{0.9}, \quad \text{ïðè } 0 < \varepsilon < 0.5;$$
$$A_{\ddot{A}} = 1 + (2.76 - 2.45\varepsilon)\overline{P}_N^{0.75}, \quad \text{ïðè } 0.5 < \varepsilon < 0.9, \qquad (25)$$

here $A_{\hat{E}}$, $B_{\hat{E}}$ – cavitation parameters of a "short" closed ends damper, $A'_{\hat{e}}$, $B'_{\hat{e}}$ – cavitation parameters of a "short" open ends damper, $A_{\ddot{A}}$ - cavitation parameters of a "long" damper, $\varepsilon = e/c$ – dimensionless eccentricity, $\overline{P}_{\hat{e}} = \overline{P}_N (R/L)^2$ – dimensionless oil supply parameter, $\overline{P}_N = \overline{P}_{\ddot{i}} - \overline{P}_{\acute{i}}$, $\overline{P}_{\ddot{i}}$ – dimensionless oil supply pressure, $\overline{P}_{\acute{i}}$ – dimensionless saturation pressure. The dimensionless pressure calculated by the equation:

$$\overline{P} = \frac{c^2 P}{12\mu\Omega R^2}. \qquad (26)$$

At $A_{\hat{E}}\,(A_{\ddot{A}}) > 2$ the cavitation does not appear, the 2π-film and the complete coverage theory may be applied. At $A_{\hat{E}}\,(A_{\ddot{A}}) < 1.1$ the π-film and the half coverage theory may be applied. At $1.1 < A_{\hat{E}}\,(A_{\ddot{A}}) < 2$ the cavitation effect may be calculated by the method [1], or by the numerical solution of the 2-D Reynolds equation with the Swift-Stieber boundary conditions, or by more advanced cavitation models.

Finally the damper clearance flow simulation may be presented in 3 levels by spatial dimensions as the following:

1) 3-D flow simulation with an analysis of maximal number of effects by means of special or general-purpose CFD codes. The advantage is the possibility to obtain a detailed flow pattern at the considered operating mode. This simulation disadvantage is the large calculation amount .
2) 2D simulation with the Reynolds equation modified or not for additional factors analysis. If the assumptions don't hurt the physical model results, the advantage is the much smaller calculation amount. The disadvantage is the limited application area, the thin film assumption requires special consideration of structural elements: oil pockets, oil supply channels and grooves. Considering of the fluid inertia in analysis is also complicated.
3) 1-D Reynolds equation. The advantages are the analytical solution for the pressure distribution and minimal calculation amount. The disadvantage are the limited application area, poorer reliability of the physical model and all restrictions of the previous method is also present.

Mathematical model application critetia

It is shown above the more complicated simulation of the fluid film flow inevitably increases the problem dimension and the calculation time. Taking into account some factors may be not reasonable because of their minor influence upon the final result. Table 1 summarizes limits for application of 1-D models and criteria for the influencing factors.

Table 1. limits of simulation models application

<table>
<tr><td rowspan="2">Flow mode</td><td colspan="2">Laminar</td><td colspan="2">Turbulent</td></tr>
<tr><td colspan="2">$Re < 1200$</td><td colspan="2">$Re > 1200$</td></tr>
<tr><td rowspan="2">Calculation method</td><td>“Short” damper</td><td colspan="2">Finite length damper</td><td>“Long” damper</td></tr>
<tr><td>$L/D < 0.5$
$\varepsilon \leq 0.75$</td><td colspan="2">$0.5 < L/D < 2$</td><td>$L/D > 2$</td></tr>
<tr><td rowspan="2">Inertia consideration</td><td colspan="2">Convective component</td><td colspan="2">Temporal component</td></tr>
<tr><td colspan="2">$\Omega_* > 10$</td><td colspan="2">$\Omega_* > 1$, unsteady problem</td></tr>
<tr><td rowspan="2">Cavitation consideration</td><td>«π - film»</td><td colspan="2">Specific account</td><td>«2π -film»</td></tr>
<tr><td>$A_{\hat{E}}$ ($A_{\ddot{A}}$) < 1.1</td><td colspan="2">$1.1 < A_{\hat{E}}$ ($A_{\ddot{A}}$) < 2</td><td>$A_{\hat{E}}$ ($A_{\ddot{A}}$) > 2</td></tr>
</table>

Table 1 shows the possibility of the analytical models application or the necessity to apply more accurate numerical solutions. The limits for 1-D and 2-D models application, consideration of turbulence and inertia are taken from the initial assumptions or experiments.

Conclusion

Mathematical models of various design squeeze film dampers based on 1-D and 2-D Reynolds equations alike are reviewed. Limits of the models applicability in rotor dynamics problems are discussed.

In the computational cost point of view, it is obvious that using of 1-D Reynolds equation analytical solutions is much more advantageous in comparison with numerical solving of 2-D Reynolds equation. In the last case, calculation time of even simple rotor systems will be greater about several orders than the analytical solution. However in some cases it is necessary to use 2-D Reynolds equation, because using SFD analytical models out of its application limits may leads to vague results.

Criteria for consideration of the influencing factors are discussed, which can be used by an engineer when choosing concrete SFD model during assembling a complete rotor system dynamic model.

References

1. Belousov A.I., Balyakin V.B., Novikov D.K. *Teoriya i proektirovanie gidrodinamicheskikh dempferov opor rotorov* [Theory and Design of hydrodynamic dampers in rotor supports]. Samara: Samarskiy Nauchnyy Tsentr RAN Publ., 2002. 335 p.
2. Leontev M. K. *Konstruktsiya i raschet dempfernykh opor rotorov GTD: Uchebnoe posobie* [Design and calculation of GTE rotors damper supports: Textbook]. Moscow: Moscow Aviation Institute Publ., 1998. 44 p.
3. Sergeev S. I. *Dempfirovanie mekhanicheskikh kolebaniy* [Damping of mechanical vibrations]. Moscow: Fizmatgiz Publ., 1959. 408 p.
4. Zeidan F. Y., San Andrés L., Vance J. M. Design and application of squeeze film dampers in rotating machinery. *Proceedings of the 25th Turbomachinery Symposium.* 1996. P. 169-188.
5. Szeri A. Z. *Fluid film lubrication.* - 2nd ed. Cambridge: Cambridge University Press, 2011. 547 p.
6. Fletcher C.A. Computational techniques for fluid dynamics. V. 1. Fundamental and general techniques. New York: Springer-Verlag, 1988. 418 p.
7. Dousti S., Gerami A., Dousti M. A numerical CFD analysis on supply groove effects in high pressure, open end squeeze film dampers. *International Journal of Engineering Innovation and Research.* 2016. V. 5, Iss. 1. P. 80-89.
8. Reynolds O. On the Theory of Lubrication and Its Application to Mr. Beauchamp Tower's Experiments, Including an Experimental Determination of the Viscosity of Olive Oil. *Proceedings of the Royal Society of London.* 1886. V. 40, Iss. 242–245. P. 191–203.
9. Zeidan F. Y., Vance J. M. Cavitation Effects on the Pressure Distribution of a Squeeze Film Damper Bearing. *Proceedings of the Texas A&M Workshop on Rotordynamic Instability Problem in High – Performance Turbomachinery.* 1988. P. 111-132.
10. Dowson D., Taylor C.M. Cavitation in bearings. *Annual Review of Fluid Mechanics.* 1979. V. 11, Iss. 1. P. 35–65.
11. San Andrés L. *Modern Lubrication Theory.* Notes 6: Cavitation in Liquid Film Bearings. Texas A&M University Digital Libraries, 2010. P. 15. Available at: http://repository.tamu.edu/handle/1969.1/93197.
12. Nelson C.C. The effect of turbulence and fluid inertia on a squeeze film bearing damper. *AIAA, SAE, and ASME, Joint Propulsion Conference, 16 th,* Hartford, Conn, 1980. P. 5.
13. San Andrés L. *Modern Lubrication Theory.* Notes 13: Squeeze Film Dampers: Operation, Models and Technical Issues. Texas A&M University Digital Libraries, 2010. P. 22. Available at: http://repository.tamu.edu/handle/1969.1/93197.
14. San Andrés L. *Modern Lubrication Theory.* Notes 4: Static Load Performance of Plain Journal Bearings. Texas A&M University Digital Libraries, 2010. P. 15. Available at: http://repository.tamu.edu/handle/1969.1/93197.

Information about authors:

Kutakov Maksim N., software engineer, Engineering & consulting centre for dynamic problems in rotating machinery Alfa-Transit, Co. Ltd. E-mail: maxim.kutakov@alfatran.com. Area of scientific interests: rotor dynamics, computational fluid dynamics.

Degtiarev Sergey A., development team leader, Engineering & consulting centre for dynamic problems in rotating machinery Alfa-Transit, Co. Ltd. E-mail: degs@alfatran.com. Area of scientific interests: rotor dynamics, vibrational diagnostics.

Leontiev Mikhail K, Doctor of science (Technical), Professor of 203 department «Construction and design of engines», Moscow aviation institute (national research university). E-mail:lemk@alfatran.com. Area of scientific interests: designing of aviation engines constructions, strength of constructions, rotor dynamics, vibrational diagnostics.